ACS APPLIED OPTICAL MATERIALS

pubs.acs.org/acsaom

Article

Enhancing Sensitivity of Mid-infrared Waveguide Spectroscopy with a High-Index Thin Film

Pontus Forsberg,* Lucas Perez, and Mikael Karlsson*

Cite This: *ACS Appl. Opt. Mater.* 2023, 1, 536−543

Read Online

ACCESS | Metrics & More | Article Recommendations

ABSTRACT: Waveguides are useful in mid-infrared spectroscopy for achieving high sensitivity on a small surface area. Here we demonstrate that by adding a thin high-index film, a highly asymmetric sensitivity enhancement can be achieved between the top and bottom of the waveguide. By enhancing the sensitivity only on the top side of the waveguide, we produced a 15 μm thick diamond waveguide on an absorbing silicon dioxide cladding. This waveguide is as sensitive as a much thinner waveguide while simplifying edge coupling of broadband light. Losses were reasonable between 5.5 and 9 μm wavelength, demonstrating that the asymmetric enhancement allows otherwise poor cladding materials to be used.

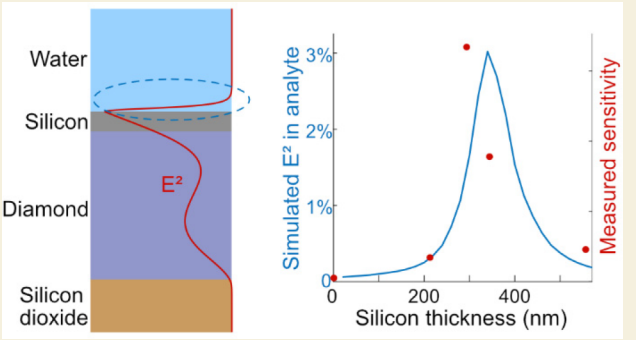

KEYWORDS: *mid-infrared, spectroscopy, diamond, waveguide, sensor, evanescent field*

1. INTRODUCTION

In this paper, we will explore the possibility of enhancing the sensitivity of waveguides used for spectroscopy by depositing a high-index film. This has previously been done for single mode slab waveguides at visible wavelengths[1] and optical fibers at visible and near-infrared wavelengths.[2,3] Here we extend it to multimode slab waveguides and mid-infrared (mid-IR) wavelengths, where for example proteins and other organic molecules have characteristic absorptions. By enhancing the sensitivity of a thick waveguide, instead of using a thin waveguide that is intrinsically more sensitive, edge coupling of broadband light is greatly simplified, and absorption in the supporting material can be reduced. This allows for example silicon dioxide (SiO_2), often used as a cladding material at near-infrared wavelengths, to be used in much of the mid-infrared even with a sensitive waveguide. The Article begins with a brief overview of waveguide spectroscopy and its relationship with attenuated total reflection (ATR) spectroscopy. We then explain the factors that affect the sensitivity of a slab waveguide and what happens when a high-index film is introduced. After this, we focus on demonstrating a simple and robust waveguide sensor consisting of a thick diamond film on SiO_2 cladding and using silicon as the high-index film. This waveguide is studied both through simulation and experiment to provide an example of how varying the thickness of the high-index film affects sensitivity.

ATR mid-IR spectroscopy is a widely used method in many fields.[4] A prism of IR transparent material (called an internal reflection element, or IRE) is put in contact with the sample. Light is coupled through the IRE and reflected off the interface with the sample at an angle that produces total reflection. While the light is reflected, there is not a sharp edge to the electromagnetic (EM) field. A field extends beyond the interface with a strength that decreases exponentially with distance. This so-called evanescent field can interact with the sample and be absorbed, hence the attenuated part of ATR. By placing or pressing the sample against the IRE, sample preparation for ATR spectroscopy can be very quick, even for solid samples. To increase the absorption in the sample, multiple reflections within the IRE can be used.

By reducing the thickness of a multireflection ATR prism, we can increase the number of reflections per unit length. At some point, the thickness is small enough that we start seeing interference effects and distinct propagating modes, and we begin thinking of the prism in terms of an optical slab waveguide (also called a planar waveguide) instead. In a thick waveguide, there are typically a large number of modes that can propagate, though in practice, light is often coupled into just one or a few of these, while for a very thin waveguide, just a single mode may be possible. Using waveguides for spectroscopy can be advantageous for several reasons: as thin

Received: September 29, 2022
Accepted: January 13, 2023
Published: January 27, 2023

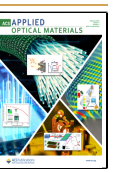

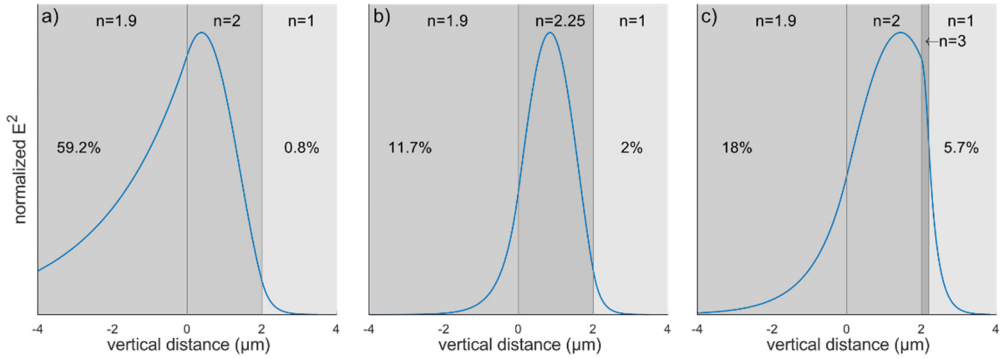

Figure 1. Illustration of the effect of refractive index on the intensity profile in a single mode waveguide. A 2 μm thick waveguide with a cladding/substrate on one side (on the left in the figures) and air on the other. Light with a wavelength of 5 μm is coupled through it. Refractive indices of the layers are shown at the top, and the percentages show the proportion of the intensity in the cladding and analyte. The blue curve shows the squared electric field, normalized to the peak value. (a) When the index difference between the cladding and waveguide is small, much of the intensity resides in the cladding and very little above the waveguide. (b) If we increase the refractive index of the waveguide, the mode is shifted upward and is more confined to the waveguide layer. The shift upward increases sensitivity, but increasing the refractive index further will further confine the mode and start reducing sensitivity. (c) The same waveguide as in (a) with a 200 nm film of a higher index material. This serves to pull the field toward the surface and gives a relatively high proportion of the intensity in the analyte. Mode profiles calculated with OMS.[7]

film devices, they may be more easily integrated on a chip, the small footprint and high sensitivity may make them suitable for integration in microfluidics, and the high surface sensitivity makes it attractive to specifically bind biomolecules to a waveguide. For these reasons, waveguides for mid-IR evanescent field spectroscopy have been studied for some time.[5,6] High sensitivity, that is, high absorbance from a low concentration of substance, in infrared spectroscopy comes with advantages and drawbacks. When studying high concentrations and large amounts of substances with strong absorptions, high sensitivity will simply mean that there is no light on the detector. In these cases, single reflection ATR spectroscopy with a high refractive index IRE may be preferable. On the other hand, if we want to study very small amounts of substance, a higher sensitivity can push the limit of detection or quantification down (given that noise is also kept low). Since the sensitivity of a waveguide used for spectroscopy scales linearly with the length, optimizing the sensitivity per unit length also allows for further miniaturization.

The sensitivity of a slab waveguide on a cladding layer depends on the proportion of the guided light that extends as an evanescent field on the analyte side, which in turn depends on several factors: The thickness of the waveguide, the refractive indices of the waveguide, cladding, and analyte, the wavelength of light, and (in the case of a multimode waveguide) which guided mode or modes are excited. The effects of these parameters can be explored with a one-dimensional mode solver, such as OMS.[7] The mode and the thickness are straightforward: The higher modes in a multimode waveguide will typically have a greater evanescent field than lower ones, so coupling light into these can give greater sensitivity. This is analogous to reducing the angle of incidence in ATR spectroscopy. A thicker waveguide will have a larger proportion of the EM field confined inside the waveguide and so will be less sensitive than a thin one. However, a very thin waveguide is usually more challenging to work with; it is often more fragile and more difficult to couple broadband light into without high losses and increased noise. The effect of the refractive index on sensitivity is more nuanced. Reducing the difference in refractive index between the waveguide and the surrounding medium gives a stronger evanescent field. In the case where the waveguide is surrounded by analyte on both sides, this means that sensitivity increases as the index of the waveguide decreases. An unsupported waveguide tends to be fragile and difficult to clean, so a supporting cladding under the waveguide is often used. If the cladding layer has a refractive index higher than the analyte, the evanescent field is stronger in the cladding than in the analyte, leading to lower sensitivity (Figure 1a). In this case, sensitivity can sometimes be improved by increasing waveguide refractive index (Figure 1b). Increasing the refractive index further will however confine the field more strongly in the waveguide and again decrease sensitivity. Instead of increasing the refractive index in the whole waveguide, a thin film of high-index material on top of the waveguide can be used to shift the field toward the analyte and away from the cladding (Figure 1c).

Sensitivity in ATR spectroscopy typically increases with increasing wavelength as the evanescent field penetrates further into the analyte. In the waveguide case, the mode profiles are wavelength dependent, which means that both the sensitivity of the individual modes and which modes are excited can change with wavelength. Refractive index is also wavelength dependent, in particular around strong absorption peaks. Since refractive index affects sensitivity, this wavelength dependence can change both the shape and position of peaks in waveguide and ATR spectroscopy compared to transmission spectroscopy.

Leaving the simple slab waveguide, there are many ways to increase sensitivity by using more complex geometries. These include making the waveguide into a narrow strip, which increases sensitivity by also having an evanescent field on the sides,[8,9] or using a subwavelength grating,[10] which essentially allows the analyte to penetrate into the waveguide. At the intersection of these is the slot waveguide, with a subwavelength slot in a strip waveguide.[11] Forming the waveguide into a narrow strip also allows for the fabrication of ring resonators and similar devices that can be used as sensors by detecting changes in resonance frequency.[9−11] All of these, especially the slot and subwavelength waveguides, require careful microfabrication with very smooth sidewalls to avoid high losses.[12] The very fine features may also be difficult to clean when fouled by sticky analytes, so they may be

https://doi.org/10.1021/acsaom.2c00108
ACS Appl. Opt. Mater. 2023, 1, 536−543

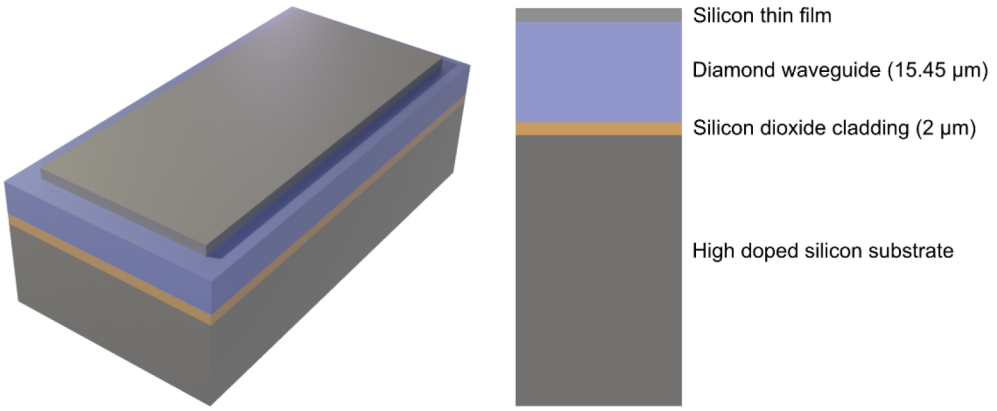

Figure 2. Schematic sketch of the waveguide; film thicknesses are exaggerated. The substrate is not included in the simulations, since the SiO_2 is thick enough to avoid interaction between the substrate and waveguide. The silicon film did not reach the edges of the waveguide; this was to avoid coupling light directly into a silicon-on-diamond waveguide. In the experiment, the lateral dimensions of the waveguide were 5 by 10 mm. Spectroscopy measurements were done along the 5 mm direction, with the 10 mm only used for loss measurements.

most suitable for sensing carefully controlled liquid samples or gases.

In this Article, we explore how a thin film of high refractive index material on top of a slab waveguide affects the sensitivity, with the goal of producing a simple and robust sensor waveguide which is easy to handle and clean. Improving the sensitivity should be possible in two cases: First, if the waveguide is thick, most of the field will reside within the waveguide and a high-index film can be used to shift it toward the surface. Second, if the cladding has a higher refractive index than the analyte, a large portion of the field may reside in the cladding; a film can then be used even on a thin waveguide to increase sensitivity (as illustrated in Figure 1). Our model system in the rest of the article is a thick (15.45 μm) diamond waveguide on SiO_2 cladding. For the high-index film, we used sputtered silicon. A sketch of the waveguide is seen in Figure 2. The sensitivity was tested with isopropyl alcohol (IPA) in water; in particular, we studied the absorption peaks around 7.25 μm (1380 cm^{-1}) and 8.62 μm (1160 cm^{-1}). SiO_2 is quite strongly absorbing at these wavelengths and as such would typically not be considered a good cladding material. We will use this to explore another potential benefit of adding a thin film on top of the waveguide: increasing sensitivity to the analyte without increasing, or even reducing, losses in the cladding.

2. SIMULATIONS

For our theoretical treatment of the waveguide, we will first look at the modes individually and then move on with two-dimensional finite difference time domain (FDTD) simulations. The refractive indices used are shown in Table 1.

Table 1. Refractive Indices Used in the Calculations

	7.25 μm	8.62 μm	Reference
Analyte (water)	1.31	1.27	13
Film (silicon)	3.42	3.42	14
Base waveguide (diamond)	2.38	2.38	15
Cladding (SiO_2)	1.04	1[a]	16

[a]In the case of SiO_2, 8.62 μm is close to the strong Reststrahlen absorption peak around 9.3 μm, and the refractive index actually drops below 1. Since absorption is not included in our calculations, a value of 1 is used.

Figure 3 shows the distribution of the intensity in the waveguide for the first two modes, calculated by finite difference method. Coupling light straight into a multimode waveguide with a vertical end face, we do not expect to excite higher modes, so we limit ourselves to looking at the first two modes here. The graphs in the center and right show the proportion of intensity (which we use as a proxy for sensitivity) in the analyte and cladding for both transverse electric (TE) and transverse magnetic (TM) modes. There are several things to note here. In the top left figure, we can see that the intensity is very high at the top of the waveguide when the silicon film reaches a certain thickness. This is due to the silicon becoming thick enough to support a mode of its own and the fundamental mode moving up to fill this position. This represents a very thin silicon-on-diamond waveguide, which can be made very sensitive. As an example, the peak intensity proportion in the analyte of the TE_0 mode at 7.25 μm wavelength (this occurs at 560 nm silicon film thickness, outside the plots in Figure 3) is about 5 times greater than that of the TE_1 mode. However, our goal here is to improve the sensitivity of a thick waveguide, not produce an ultrathin waveguide, so we will avoid coupling light into the silicon film directly. In the lower left figure, we see that the first mode also shifts higher as the silicon thickness increases. One intensity peak moves up to the surface and then weakens, while the other widens to resemble the fundamental mode in the plain diamond waveguide. Comparing the intensities in the analyte of the fundamental and first mode, we see that the points where they cross coincide almost perfectly with a peak in the intensity in the first mode. This point also coincides with the minimum thickness at which the silicon film can support a guided mode. So, as the thickness increases from this point, the fundamental mode represents a thin silicon-on-diamond waveguide, and at the same time, the first mode loses intensity in the analyte. This means that if we couple light into the diamond layer, we would expect a peak in sensitivity when the silicon film is just thick enough to support a mode of its own. Comparing the TE and TM modes, we note three things: First, the TM modes require a thicker silicon film than the TE modes to see a similar effect. This is expected, since a slab waveguide has to be thicker to support a TM mode. Second, the peak intensity of the first mode is nearly the same for the TE and TM modes, while the intensity without a silicon film is higher for the TM mode. Third, the TM modes are stronger in

https://doi.org/10.1021/acsaom.2c00108
ACS Appl. Opt. Mater. 2023, 1, 536−543

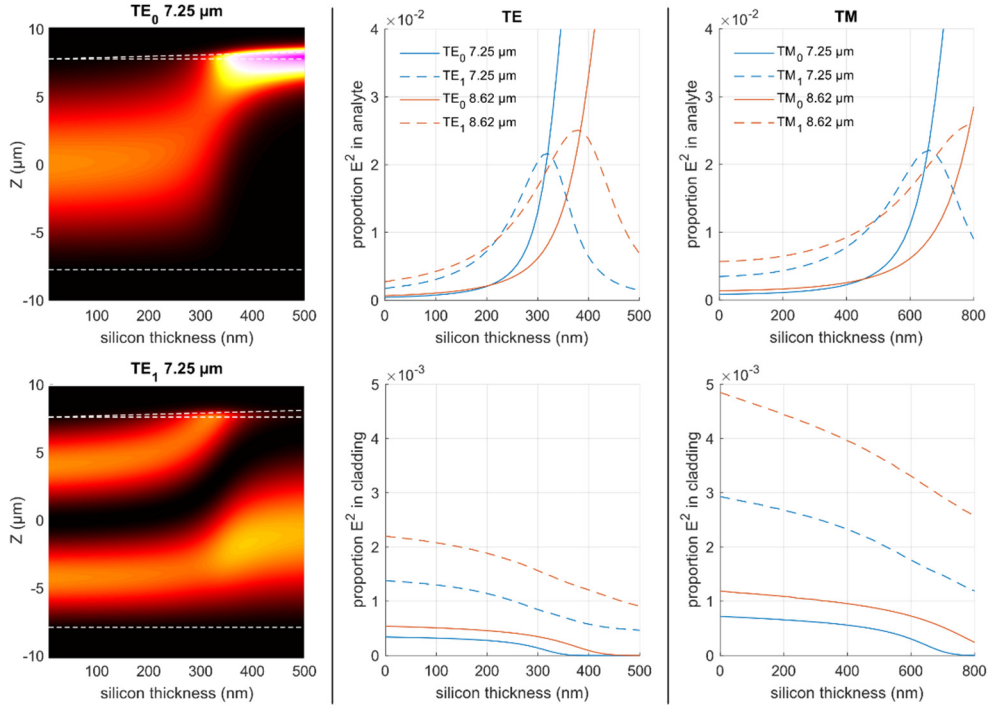

Figure 3. Mode solver results for a 15.45 μm thick diamond waveguide on SiO_2 with a varying thickness of silicon on top. Left: Vertical distribution of intensity of the lowest two TE modes at 7.25 μm wavelength. The dashed lines show the positions of the interfaces. Center and right: The proportion of power in the analyte and cladding. The proportion in the analyte (water) is shown in the top graphs, and the proportion in the cladding is shown in the bottom graphs (note that the *Y*-axis exponent is different). TE modes are in the center, and TM modes are on the right. The fundamental modes are plotted as solid lines; first higher modes as dashed. Blue lines show 7.25 μm wavelength, and red lines show 8.62 μm wavelength.

Table 2. Comparison of the Proposed Design and Several Slab and Strip Waveguides from the Literature Using a 1D Mode Solver for the TM_0 Mode[a]

Reference	Material	Thickness	Wavelength	n1	n2	n3	E^2 in water
17	Ge on Si	3 μm	10 μm	3.42	4.00	1.22	2.6%
18	GaAs on AlGaAs	6 μm	9.1 μm	3.2	3.3	1.26	0.36%
19	Chalcogenide (GeSbSe)	1.7 μm	7.7 μm	2.44	2.77	1.30	4.3%
20	Diamond on AlN	5 μm	7.25 μm	1.88	2.38	1.31	1.8%
21	Ge on Si	2 μm	5.8 μm	3.42	4.01	1.29	1.95%[b]
	Diamond on SiO_2	15.45 μm	7.25 μm	1.04	2.38	1.31	0.085%
			8.62 μm	1	2.38	1.27	0.14%
	Diamond on SiO_2 with Si film	15.45 μm	7.25 μm	1.04	2.38/3.42	1.31	2.2%[c]
			8.62 μm	1	2.38/3.42	1.27	2.6%[c]

[a]n1, n2, and n3 are the refractive indices of substrate, guiding layer and water respectively. [b]This strip waveguide has a width close to the thickness, while this comparison only compares the field on top of the waveguide, so the actual proportion of electric field in the analyte is likely higher (the other waveguides in this comparison have widths much greater than the thickness). [c]With optimized Si film thickness (where the lines cross in the upper right graph of Figure 3). Since most waveguides in the literature use TM polarization, this is what we compare here. In this paper, we focused on the TE modes, in which case these values are instead 2.2 and 2.5%.

the cladding than the TE modes. Taken together, this means that we expect lower losses and a proportionally greater effect of the silicon film in the TE polarization, so we will focus on this from here on. Comparing the two wavelengths, we can see that the crossover point shifts proportionally with wavelength. Finally, looking at the lower graphs in Figure 3, we see that the intensity in the cladding goes down moderately with increased film thickness. However, if we couple light into the diamond layer, we expect to start coupling more light into the first mode as the fundamental mode moves into the silicon film. It therefore seems likely that sensitivity to the cladding will first drop somewhat before increasing as the film thickness passes this point.

In order to give the reader a frame of reference for the proportion of power in the analyte, Table 2 shows a similar mode calculation made for several slab and strip waveguides from the literature. For simplicity, the strip waveguides have been treated as slabs, which is a good approximation as long as the waveguide is significantly wider than it is thick, which is true for all but one of the waveguides in the table. As can be seen, the diamond waveguide with a silicon film can reach a similar level of sensitivity while being by far the thickest waveguide in the table. Only the chalcogenide waveguide in reference 19 is significantly more sensitive, and this waveguide is nearly an order of magnitude thinner.

https://doi.org/10.1021/acsaom.2c00108
ACS Appl. Opt. Mater. 2023, 1, 536−543

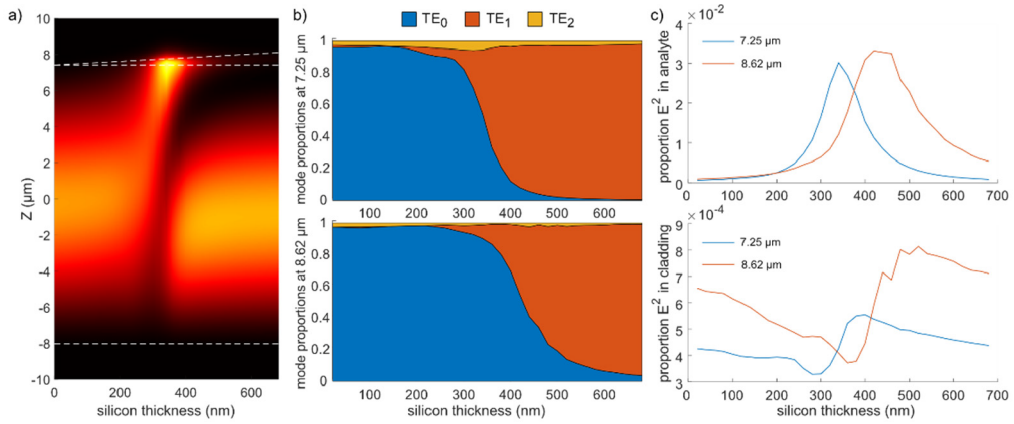

Figure 4. FDTD simulation results and fits of mode profiles. (a) Vertical intensity distribution of 7.25 μm wavelength in diamond waveguides with a varying thickness of silicon on top. Dashed lines show the interfaces. (b) Proportions of the first three mode profiles that give the best fit to the intensity profile for each film thickness (in steps of 20 nm). The resolution of the FDTD computational grid was 40 nm, which was not enough to resolve small differences in film thickness. The subpixel averaging in MEEP overcame this to some extent, but to further improve the fit, the mode profiles for thicknesses within 5 nm were fitted to the intensity profile at each simulated thickness, and the thickness with the best fit was used. (c) The intensity proportion in the analyte and cladding corresponding to the mode proportions in (b).

The mode calculations have shown the film thickness range that is likely to be most relevant; we now turn to 2D FDTD simulations to see how a focused beam actually couples into the diamond waveguide and how a silicon film changes the intensity of the evanescent field. For this, we used MEEP[22] to simulate a 700 μm long waveguide with the same thickness and refractive indices as above. A Gaussian beam with a waist radius of 5 μm was focused on one end. There was no silicon film on the first 100 μm of the waveguide to avoid coupling light into the film directly. To get the intensity profile, the squared electric field was averaged along the latter part of the waveguide. Figure 4a shows the intensity profiles for 7.25 μm wavelength as the silicon film increases in thickness. We can see how the intensity first shifts toward the surface and then starts coupling into a higher mode. A peak in the evanescent field is clearly seen around this transition. By fitting the previously calculated mode profiles to the intensity profiles, we can extract the proportion of light in the different modes (Figure 4b). It is clear that as the fundamental mode becomes that of a silicon waveguide on diamond, the proportion in this mode drops rapidly. This results in a peak in the evanescent field in the analyte around this point (Figure 4c) which is somewhat higher than that of the TE_1 peak in Figure 3 since some light is still in the TE_0 mode.

While the peak in the evanescent field is fairly narrow, there is still a lot of overlap for the two wavelengths studied here. So, while maximum sensitivity enhancement from a high-index film is only possible for a narrow wavelength band, a wide band will see significant enhancement. We now turn to a practical test of this waveguide geometry, to see how much we can increase the sensitivity.

3. EXPERIMENT

3.1. Waveguide Fabrication

A 2 μm thick SiO_2 film was grown by thermal wet oxidation (1050 °C) on a 5 mm thick, highly n-type phosphorus doped silicon wafer (2.081×10^{19} cm^{-3}). Polycrystalline diamond of optical quality was deposited on the wafer and polished by Diamond Materials GmbH, who also polished the silicon down to 0.5 mm thickness. The diamond thickness was close to 15 μm across the wafer. The wafer was divided into smaller waveguide samples (5×10 mm^2) by laser cutting. The samples chosen for the current study had a diamond thickness of 15.45 μm. All four edges of the waveguide were mechanically polished on a CVD-diamond-coated polishing wheel (Nova Diamant AB). The diamond adhesion to the SiO_2 was rather poor, and there was some limited delamination in the corners of the sample. Samples were prepared both with vertical edges and edges angled at approximately 40°. The angled edges allowed coupling light into higher modes in the waveguide. These higher modes were however too sensitive to absorption in the SiO_2 cladding to make the waveguide useful, so only the vertical edge sample was used for the spectroscopy experiments.

The silicon film was deposited on top of the waveguide by sputtering in a Von Ardenne magnetron sputter system (500 W pulsed DC power in 1.5 μBar argon atmosphere). A 3D-printed frame covered the edges of the sample during sputtering. The frame covered around 200 μm along the edge, and shadowing effects during sputtering then gave a gradual increase in the thickness over around 300 μm, so that full thickness was reached approximately 500 μm from the edge. This was done so that the coupling of light into the waveguide should not be affected by the silicon film. After optical measurements, the film thickness was increased by further sputtering. A test sample, masked with a thin adhesive tape, was sputtered together with the waveguide each time, in order to measure the thickness of the sputtered silicon. Thickness was measured with stylus profilometry (Veeco Dektak 150) and interferometry (Zygo Nexview NX2). The film thicknesses used in this study were 210, 290, 340, and 550 nm. These were chosen to sample the region of interest indicated by the simulations above, with one thickness well below the sensitivity peak, two close to the peak for the 7.25 μm wavelength, and the thickest silicon film chosen to be close to the peak in sensitivity of a silicon-on-diamond waveguide.

3.2. Optical Testing

Our waveguide spectroscopy setup is shown schematically in Figure 5. The tunable QCL used to test the waveguides was a MIRcat system from Daylight Solutions. Two gold mirrors were used to steer the beam, while a half wave plate and two linear polarizers were used to control intensity and polar-

https://doi.org/10.1021/acsaom.2c00108
ACS Appl. Opt. Mater. 2023, 1, 536−543

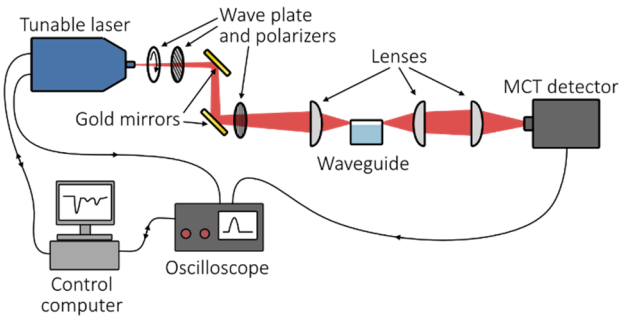

Figure 5. Schematic illustration of the setup for waveguide spectroscopy.

ization. The beam was focused onto one end of the waveguide by a 12.5 mm lens, while the output was gathered by a 12.7 mm lens, and a 25 mm lens focused it on the thermoelectrically cooled MCT detector (VIGO System PVMI-4TE-12). Alignment and focus were adjusted by maximizing the detector signal. The signals from the detector, as well as trigger signals from the laser, were recorded by a National Instruments PXIe-5114 oscilloscope. A LabView script controlled the laser and oscilloscope to collect the spectra.

The QCL system contains four modules that together cover a spectral range between 1900 and 900 cm^{-1} (5.3−11.1 μm) The whole range was used for the loss measurements, while the sensitivity measurements were made with a single module (1453−1133 cm^{-1}, 6.88−8.83 μm).

The sensitivity of the waveguide was measured for each silicon film thickness by collecting spectra of several concentrations of IPA in water. This was done using the shorter dimension of the waveguide (5 mm). The liquid was placed as a droplet on top of the waveguide, covering the entire length. The concentrations used were (in vol%) 0, 5, 10, 15, 20, and 25, and each concentration was measured twice. Spectra were measured by scanning the QCL across the range five times; each scan took 5 s, and the reset time for the next scan was 10 s, so the time from the start of the first scan to the end of the last scan was 65 s, which was short enough that no change in the IPA concentration from evaporation was seen. Background spectra of pure water were measured in the same way before each sample measurement.

Propagation losses were measured by passing light through the waveguide along both the shorter (5 mm) and longer (10 mm) dimensions of the waveguide. Assuming coupling losses to remain the same, the propagation loss in dB/cm can be calculated as $-20 \times \log_{10}(V_{10}/V_5)$, where V_{10} and V_5 are the measured output powers with the 10 and 5 mm waveguides respectively. Focus and position was adjusted for each measurement to maximize the signal on the detector, and the measurements were repeated at least twice for each wavelength.

After spectra had been collected with the thickest film on the waveguide, the silicon was stripped by placing droplets of a mixture of hydrofluoric acid and nitric acid on top of the waveguide. First, only part of the waveguide was stripped so that the thickness of the silicon film could be verified, then the rest of the silicon film was removed, and spectra were measured again to ensure that the waveguide was not damaged during the handling and processing.

3.3. Results

Transmittance spectra (measured power on the detector with sample divided by the pure water background) are shown in Figure 6 for the plain diamond waveguide as well as with two of the thicknesses of silicon film. We can immediately see that the increased absorption in the analyte with the silicon film on the waveguide gives rise to smoother spectra. Also note how the wavelength dependent sensitivity enhancement can drastically alter the relative intensity of the absorption peaks. Below the spectra in Figure 6 are plots of absorbance for the peaks at 7.25 μm (1380 cm^{-1}, the stronger peak in the double peak is used) and 8.62 μm (1160 cm^{-1}) against IPA concentration, with linear fits to the data. The slope of the line represents the sensitivity of the waveguide to the respective absorption peak. Looking at the sensitivity for all the film thicknesses (Figure 7a), we can see that qualitatively

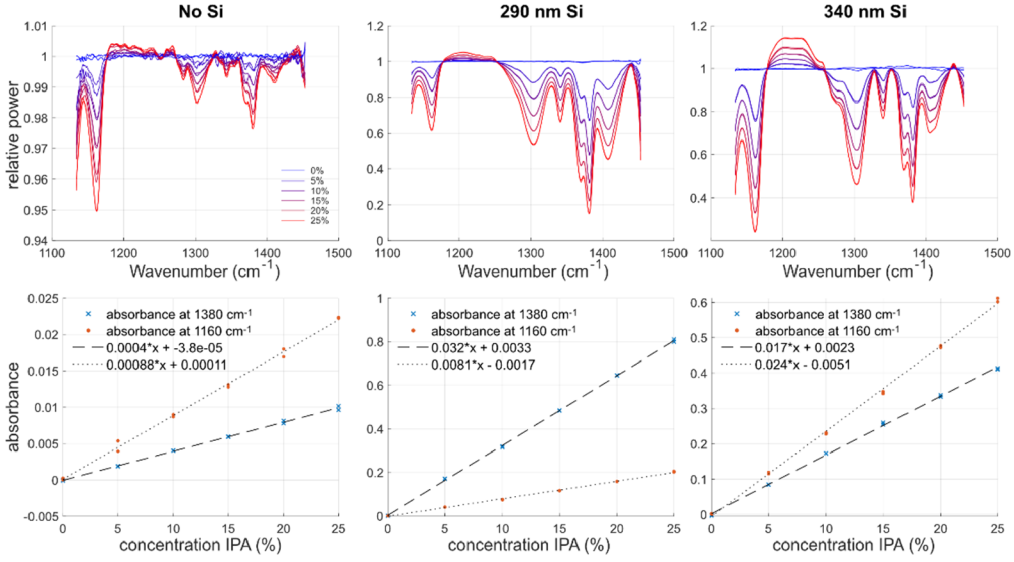

Figure 6. Top row: Transmittance spectra of IPA in water. Concentration ranges from 0% (blue) to 25% (red) in increments of 5%. Bottom row: Absorbance plotted against concentration for the absorption peaks around 1160 cm^{-1} (8.62 μm) and 1380 cm^{-1} (7.25 μm). The sensitivity is the slope of the fitted line.

https://doi.org/10.1021/acsaom.2c00108
ACS Appl. Opt. Mater. 2023, 1, 536−543

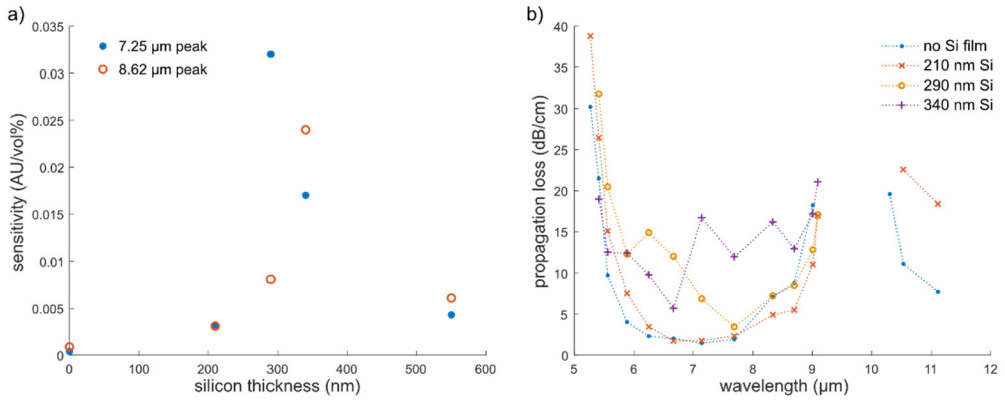

Figure 7. (a) Sensitivity of the 5 mm long waveguide to the two absorption peaks of IPA at 7.25 and 8.62 μm plotted against the thickness of the silicon film on top of the waveguide. The enhancement of the 7.25 μm peak with a 290 nm Si film, compared with the plain 15.45 μm thick diamond waveguide, was a factor of 80. (b) Measured propagation loss in the waveguide with different thicknesses of Si film.

the results agree well with the simulations. Sensitivity increases with film thickness before peaking and then decreasing again, and the sensitivity at the shorter wavelength peaks at a thinner film thickness. The sensitivity seems to peak a bit sooner than predicted, since the highest sensitivity measured for the absorption at 7.25 μm was measured with the 290 nm film rather than 340 nm. This could be due to the actual refractive indices not quite matching those used in the calculations or because the beam coupled into the waveguide was not in reality a perfectly focused and centered Gaussian beam. The beam was also adjusted each time the waveguide was put in the measurement setup to give the maximum signal on the detector, which is different from the simulated case where the beam was kept fixed for all film thicknesses. The highest sensitivity enhancement measured, compared to the waveguide with no silicon film, was a factor of 80.

The results of the propagation loss measurement are shown in Figure 7b. The high losses at the shortest wavelengths are due to absorption in the diamond waveguide, and the gap in the measurement around 10 μm wavelength is due to the refractive index in the SiO_2 cladding peaking there so that there is no waveguiding in the diamond. Compared to the case with no film, 210 nm silicon film increased losses at low wavelengths while reducing them between 8 and 9 μm while being about the same as for no film around 7 μm. This is consistent with the results in Figure 4c for the calculated intensity in the cladding layer. As the film thickness was increased, losses increased first at short wavelengths and then at longer. Again, this is consistent with the increase in intensity in the cladding as more light is coupled into the TE_1 mode. At the longest wavelengths (above 10 μm), losses increased rapidly with the applied film, perhaps due to absorption in the sputtered silicon. While a loss of 20 dB/cm is fairly high, the power of the QCL light source together with the thickness of the waveguide made it easy to couple enough light through it to get good spectra up to ~9 μm wavelength.

4. CONCLUSION

We can conclude that a high-index film on top of a slab waveguide is a practical way to increase the sensitivity when using the waveguide for mid-IR spectroscopy. Such a film can increase the sensitivity of thick waveguides, and thin waveguides resting on a cladding material with a higher refractive index than the analyte. Care must be taken to adapt the film thickness to the wavelength range of interest so that the sensitivity enhancement is optimized. Since the enhancement is wavelength dependent, the relative strengths of absorption peaks will be affected, so care should also be taken when comparing with spectra acquired with other methods (this is true in general for ATR and waveguide spectroscopy but especially so here).

Using sputtered silicon film on a diamond waveguide, the waveguide could relatively quickly be optimized for a specific wavelength band. Since diamond is extremely chemically resistant, the silicon film can easily be removed and replaced if scratched or if a different thickness is desired. With the highest enhancement demonstrated here, the sensitivity of a 15.45 μm thick diamond on SiO_2 waveguide reached 0.032 AU/vol% for IPA in water. This is a factor of 80 higher than the waveguide without a silicon film and very similar to the sensitivity of our previously demonstrated 5 μm thick diamond on aluminum nitride waveguide (0.033 AU/vol%), which could be used to measure acetone in heavy water at a concentration of 7.6 mmol/L.[20] It is also more sensitive than previous GaAs and diamond slab and strip waveguides that have been used to measure small amounts of substance.[23] This shows that a thick multimode waveguide can be pushed to a competitive sensitivity with the addition of a thin high-index film. An ultrathin silicon-on-diamond waveguide could in simulations reach a sensitivity around 4 times higher than that of the thick diamond waveguide with silicon film. In our experience however, using a thicker waveguide offers a number of practical advantages, such as easier and faster coupling of light into the waveguide and resistance to errors due to vibrations, pointing jitter, or drift.

We have also demonstrated that sensitivity can be improved asymmetrically, so that losses in the cladding are kept small. A film thick enough to optimize sensitivity to the analyte also increased sensitivity to the cladding somewhat, but to a much lesser extent. The simulations showed up to 70 times higher power in the analyte than in the cladding. This allowed us to use SiO_2 as cladding in a wavelength range where it is strongly absorbing. Other ways of increasing sensitivity—such as coupling into higher modes or reducing the thickness—give a more symmetric increase in both analyte and cladding. In general, loosening the material requirements on the cladding material may make it easier to integrate a waveguide on a chip. By patterning the sputtered film, one might also define the sensing area of the chip by increasing sensitivity locally.

https://doi.org/10.1021/acsaom.2c00108
ACS Appl. Opt. Mater. 2023, 1, 536−543

The design is of course not limited to the materials used here. A high-index thin film could be used to improve sensitivity of many suggested waveguide spectroscopy platforms,[5,6] though if the waveguide refractive index is already very high, such as for germanium, it may be difficult to find a suitable material. On a less resistant material than diamond, such as gallium arsenide or zinc selenide, the film would be more difficult to remove, but on the other hand, it could serve a dual purpose as a protective layer on the waveguide.

AUTHOR INFORMATION

Corresponding Authors

Pontus Forsberg − *Department of Materials Science and Engineering, Uppsala University, 751 03 Uppsala, Sweden;* orcid.org/0000-0002-1036-5957; Email: pontus.forsberg@angstrom.uu.se

Mikael Karlsson − *Department of Materials Science and Engineering, Uppsala University, 751 03 Uppsala, Sweden;* orcid.org/0000-0002-2011-0851; Email: mikael.karlsson@angstrom.uu.se

Author

Lucas Perez − *Department of Materials Science and Engineering, Uppsala University, 751 03 Uppsala, Sweden*

Complete contact information is available at: https://pubs.acs.org/10.1021/acsaom.2c00108

Notes

The authors declare no competing financial interest.

ACKNOWLEDGMENTS

The authors would like to thank Dr. Patrik Hollman at Nova Diamant AB for help with the polishing of the waveguides. Myfab is acknowledged for access to the nanofabrication laboratory at Uppsala University. The research leading to these results has received funding from the Swedish Research Council (VR, research grant No. 621-2014-5959).

REFERENCES

(1) Quigley, G. R.; Harris, R. D.; Wilkinson, J. S. Sensitivity enhancement of integrated optical sensors by use of thin high index films. *Appl. Opt.* **1999**, *38*, 6036−6039.

(2) Canning, J.; Padden, W.; Boskovic, D.; Naqshbandi, M.; de Bruyn, H.; Crossley, M. J. Manipulating and controlling the evanescent field within optical waveguides using high index nanolayers. *Opt. Mater. Express* **2011**, *1*, 192−200.

(3) Renoirt, J.-M.; Zhang, C.; Debliquy, M.; Olivier, M.-G.; Mégret, P.; Caucheteur, C. High-refractive-index transparent coatings enhance the optical fiber cladding modes refractometric sensitivity. *Opt. Express* **2013**, *21*, 29073−29082.

(4) Fringeli, U. P. ATR and Reflectance IR Spectroscopy, Applications. *Encyclopedia of Spectroscopy and Spectrometry* **2017**, 115−129.

(5) Schädle, T.; Mizaikoff, B. Mid-Infrared Waveguides: A Perspective. *Appl. Spectrosc.* **2016**, *70*, 1625−1638.

(6) Mittal, V.; Mashanovich, G. Z.; Wilkinson, J. S. Perspective on Thin Film Waveguides for on-Chip Mid-Infrared Spectroscopy of Liquid Biochemical Analytes. *Anal. Chem.* **2020**, *92*, 10891−10901.

(7) 1-D mode solver for dielectric multilayer slab waveguides. https://www.computational-photonics.eu/oms.html (accessed August 2022).

(8) Chang, Y.-C.; Wägli, P.; Paeder, V.; Homsy, A.; Hvozdara, L.; van der Wal, P.; Di Francesco, J.; de Rooij, N. F.; Herzig, H. P. Cocaine detection by a mid-infrared waveguide integrated with a microfluidic chip. *Lab Chip* **2012**, *12*, 3020−3023.

(9) Zhang, K.; Böhm, G.; Belkin, M. A. Mid-infrared microring resonators and optical waveguides on an InP platform. *Appl. Phys. Lett.* **2022**, *120*, 061106.

(10) Flueckiger, J.; Schmidt, S.; Donzella, V.; Sherwali, A.; Ratner, D. M.; Chrostowski, L.; Cheung, K. C. Sub-wavelength grating for enhanced ring resonator biosensor. *Opt. Express* **2016**, *24*, 15672−15686.

(11) Lvovich Kazanskiy, N.; Nikolaevna Khonina, S.; Butt, M. A. Subwavelength Grating Double Slot Waveguide Racetrack Ring Resonator for Refractive Index Sensing Application. *Sensors* **2020**, *20*, 3416.

(12) Kita, D. M.; Michon, J.; Johnson, S. G.; Hu, J. Are slot and subwavelength grating waveguides better than strip waveguides for sensing? *Optica* **2018**, *5*, 1046−1054.

(13) Hale, G. M.; Querry, M. R. Optical Constants of Water in the 200-nm to 200-μm Wavelength Region. *Appl. Opt.* **1973**, *12*, 555−563.

(14) Chandler-Horowitz, D.; Amirtharaj, P. M. High-accuracy, midinfrared (450 $cm^{-1} \leq \omega \leq$ 4000 cm^{-1}) refractive index values of silicon. *J. Appl. Phys.* **2005**, *97*, 123526.

(15) Zaitsev, A. M. *Optical Properties of Diamond: A Data Handbook*; Springer, 2001.

(16) Kischkat, J.; Peters, S.; Gruska, B.; Semtsiv, M.; Chashnikova, M.; Klinkmüller, M.; Fedosenko, O.; Machulik, S.; Aleksandrova, A.; Monastyrskyi, G.; Flores, Y.; Masselink, W. T. Mid-infrared optical properties of thin films of aluminum oxide, titanium dioxide, silicon dioxide, aluminum nitride and silicon nitride. *Appl. Opt.* **2012**, *51*, 6789−6798 Numerical values of n were accessed through the Refractive index database https://refractiveindex.info/ (accessed August 2022).

(17) Mittal, V.; Devitt, G.; Nedeljkovic, M.; Carpenter, L. G.; Chong, H. M. H.; Wilkinson, J. S.; Mahajan, S.; Mashanovich, G. Z. Ge on Si waveguide mid-infrared absorption spectroscopy of proteins and their aggregates,. *Biomed. Opt. Express* **2020**, *11*, 4714−4722.

(18) Sieger, M.; Haas, J.; Jetter, M.; Michler, P.; Godejohann, M.; Mizaikoff, B. Mid-Infrared Spectroscopy Platform Based on GaAs/AlGaAs Thin-Film Waveguides and Quantum Cascade Lasers,. *Anal. Chem.* **2016**, *88*, 2558−2562.

(19) Gutierrez-Arroyo, A.; Baudet, E.; Bodiou, L.; Lemaitre, J.; Hardy, I.; Faijan, F.; Bureau, B.; Nazabal, V.; Charrier, J. Optical characterization at 7.7 μm of an integrated platform based on chalcogenide waveguides for sensing applications in the mid-infrared. *Opt. Express* **2016**, *24*, 23109−23117.

(20) Forsberg, P.; Hollman, P.; Karlsson, M. High sensitivity infrared spectroscopy with a diamond waveguide on aluminium nitride,. *Analyst* **2021**, *146*, 6981−6989.

(21) Chang, Y.-C.; Paeder, V.; Hvozdara, L.; Hartmann, J.-M.; Herzig, H. P. Low-loss germanium strip waveguides on silicon for the mid-infrared,. *Opt. Lett.* **2012**, *37*, 2883−2885.

(22) Oskooi, A.; Roundy, D.; Ibanescu, M.; Bermel, P.; Joannopoulos, J. D.; Johnson, S. G. MEEP: A flexible free-software package for electromagnetic simulations by the FDTD method,. *Comput. Phys. Commun.* **2010**, *181*, 687−702.

(23) Wang, X.; Karlsson, M.; Forsberg, P.; Sieger, M.; Nikolajeff, F.; Österlund, L.; Mizaikoff, B. ″Diamonds Are a Spectroscopist's Best Friend: Thin-Film Diamond Mid-Infrared Waveguides for Advanced Chemical Sensors/Biosensors,″. *Anal. Chem.* **2014**, *86*, 8136−8141.